

Fibre Bragg Grating Filters for Optical Communications

I. Abe¹, O. Frazão², P. S. André^{3,4}, J. C. Cardozo da Silva¹, H. J. Kalinowski¹,
J. L. Fabris¹, J. L. Pinto^{3,4}, F. M. Araújo^{2,5}.

¹ Centro Federal de Educação Tecnológica do Paraná, 80230-901 Curitiba, Brazil.

² INESC Porto – UOSE, Rua Campo Alegre 687, 4169-007 Porto, Portugal.

³ Instituto de Telecomunicações – Pólo de Aveiro, Campus Universitário de Santiago, 3810-193 Aveiro, Portugal.

⁴ Departamento de Física da Universidade de Aveiro, Campus Universitário de Santiago, 3810-193 Aveiro, Portugal.

⁵ Departamento de Física da FCUP, Rua Campo Alegre 687, 4169-007 Porto Portugal.

Abstract

Several steps in the development of Fibre optic Bragg grating for application in tuneable wavelength devices intended to DWDM are presented.

Keywords: Fibre Bragg gratings, Optical Fibre, Optical Filter, Fabrication, phase-mask, Networking.

I. INTRODUCTION

The significant discovery of photosensitivity in optical fibres lead to the development of a new class of in-fibre component, called the fibre Bragg grating (FBG).

Fibre Bragg gratings are revolutionising the telecommunications technology due to their intrinsic integration with fibres and the large number of device functionalities that they can facilitate, such as filtering, chromatic dispersion compensation, and gain flattening. The most distinguishing feature of the FBG is the flexibility that they offer for achieving desired spectral characteristics, due to the broad range of variation in their determining physical parameters [1].

In this work we present experimental, and simulated results of the FBG filtering characteristics, and we also

study the optical spectra of a specific FBG written for selective and tuneable spectral filtering.

II. THEORY FBG

Basically a Bragg grating is a longitudinal periodically modulated refractive index profile in the core of an optical fibre (see Figure 1).

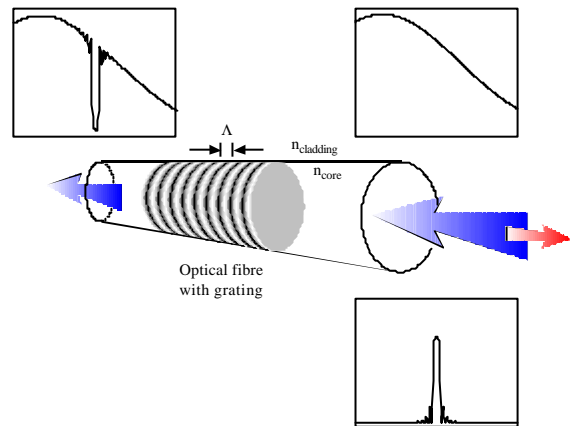


Fig. 1 – Schematic representation of a fibre Bragg Grating.

Due to that modulation, it presents a reflection band centred at the Bragg wavelength $\lambda_B = 2n_{\text{eff}} \Lambda$, being n_{eff} the effective index and Λ the period of the grating. There are two main methods: to shift the Bragg grating central wavelength peak by modifying the fibre refractive index or by changing the grating period. These variations can be dynamically induced either by temperature or by mechanical stress. The strain response arises due to both the physical elongation of the grating and the change in fibre index due to the photo elastic effect; whereas the thermal response arises due to the thermal expansion of the fibre material and temperature dependence of the refractive index. The first allows a broad tuning range (>36 nm) and high tuning speed (>10 ms/nm), but has low reproducibility and low reversibility. On the other hand, thermal tuning presents high reproducibility, high reversibility and built-in

I. Abe, J. C. Cardozo da Silva, H. J. Kalinowski and J. L. Fabris are with CEFET-PR, 80230-901 Curitiba, Brazil, Tel: +55.41.3104689, Fax: +55.41.3104683. ildabe@cpgei.cefetpr.br, cardozo@cpgei.cefetpr.br, hjkalin@cpgei.cefetpr.br, fabris@cefetpr.br.

O. Frazão and F. M. Araújo are with INESC Porto - UOSE, Rua Campo Alegre 687, 4169-007 Porto, Portugal. Tel: +351-226082601, Fax: +351-226082799. ofraza@inescporto.pt, fmaraujo@goe.fc.up.pt.

P. S. André and J. L. Pinto are with Instituto de Telecomunicações – Pólo de Aveiro, Campus Universitário de Santiago, 3810-193 Aveiro, Portugal. Tel: +351-234377900, Fax: +351-234377901. pandre@av.it.pt, ilp@fis.ua.pt.

This work was supported by the CAPES/ICCTI agreement through the *Redes de Bragg* project, by the Portuguese scientific program PRAXIS XXI (PRAXIS XXI/BD/17227/98) through the DAWN project, and by Portugal Telecom Inovação through the O-NODE project (P114). The authors also wish to thank to the INESC Porto, Centro Federal de Educação Tecnológica do Paraná, Instituto de Telecomunicações and to the Universidade de Aveiro.

temperature compensation, but it is limited by a narrow tuning range (~ 1 nm) and a low tuning speed (~ 1 s/nm).

III. GRATING FABRICATION

Essentially, there are two main methods to fabricate FBGs namely the two-beam interferometer method and the phase mask method. The first uses an interferometer to generate the optical fringe pattern necessary to writing the grating structure into the fibre core. The second process uses a phase mask (diffractive element) to generate the fringe pattern, being the fibre positioned just in contact with the phase mask surface (see Figure 2).

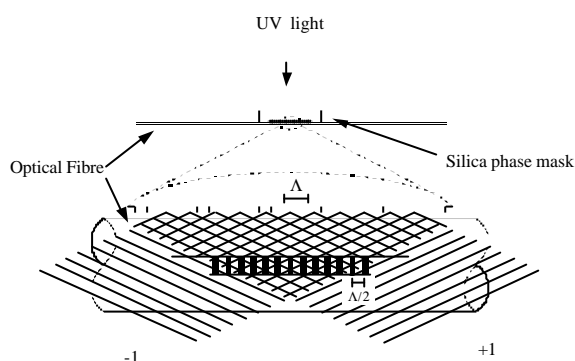


Fig. 2 – Schematic diagram of the phase mask writing process.

While the first method is more flexible to adjust the spatial characteristics of the refractive index profile written in the fibre, the second one has several advantages which include: The Bragg wavelength of an FBG is determined by the pitch of phase mask and is independent of wavelength of the UV laser; the phase mask method offers a high potential for mass production with good repeatability at low cost; this single beam writing method improves the mechanical stability of the FBG writing apparatus; the requirement for the coherence of the UV laser is reduced and hence low spatial and temporal coherence excimer lasers can be used.

The grating used in this work was manufactured by illuminating an optical fibre exposed to a phase-mask spatially modulated UV (248 nm) writing beam originated from a KrF excimer laser. The optical fibre (standard single mode type) has been previously kept under high-pressure hydrogen atmosphere in order to enhance its photosensitivity due to hydrogen diffusion into the glass matrix. This process is reliable and gives excellent results in the reduction of the writing time of the grating.

Optical characterizations after the writing revealed a reflection band centred at 1548 nm with full width half maximum of 0.3 nm. The grating was covered with a polymeric resin for protection and then bonded inside an aluminium tube (external diameter 1mm, wall thickness 0.1mm). The lead fibre lengths were protected by sheath and tubing material and finally mounted in FC/PC fibre connectors. The Aluminium tube with the grating inside

was assembled over a thermoelectric Peltier element, so that its temperature could be easily set and controlled.

IV. RESULTS

We present a hybrid method based on a thermal-stress thermally enhanced actuation on a FBG, to tune its central wavelength. The enhancement of the temperature sensitivity of wavelength in this configuration arises from the use of an Aluminium tube to which the FBG is bonded, that has a positive thermal expansion coefficient.

The faster temperature dependence and easy management of the grating peak are required for devices intended to dynamically allocated wavelength multiplexed networks, such as tuneable filters, optical add-drop multiplexers, wavelength converters.

The Optical spectra of the FBG was measured by an Anritsu MS-9710B Optical Spectrum Analyser with 0.07 nm resolution. Grating spectra was also measured with an hybrid Michelson Interferometer [2], the acquired interferograms are transformed with a Fast Fourier Transform routine to obtain the associated frequency spectra. As optical sources to illuminate the FBG either an ELED (75 nm FWHM) or the Amplified Spontaneous Emission of an EDFA were used. Light reflected by the grating is fed to the measuring apparatus through an optical coupler. Care was taken to index match the unused ports of the grating fibre and of the optical coupler, to avoid light reflected at the fibre – air interface.

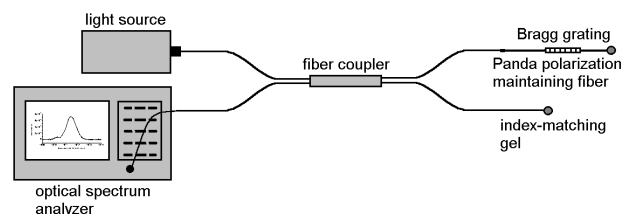


Fig. 3 – Basic Fibre Bragg grating systems measurement.

First results with the grating revealed a single band optical spectrum at room temperature, however, this spectrum presented a split when the temperature increased. Further measurements showed that after splitting the peak at higher wavelengths shifted with higher rate, followed by the peak at lower wavelength after an initial delay. After temperature stabilization both peaks collapsed again.

A second set of optical spectra of the grating at different temperatures is shown in Figure 4, taken a few months after. At room temperature two peaks are clearly identified, with peak wavelength of 1547.81 nm and 1547.99 nm, respectively, and individual FWHM of 0.20 nm. As temperature increases, the peak on the right of the spectrum shifts to longer wavelengths with a measured slope of 0.035 nm/K. The peak on the left starts to shift with the same slope, but soon that shift becomes undistinguishable as the

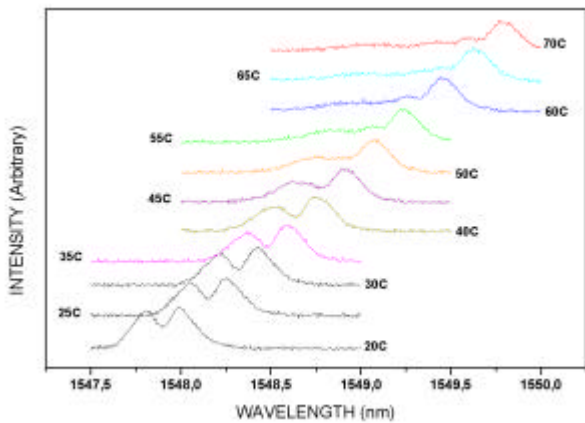


Fig. 4 – Spectral response of the FBG at different temperature.

reflection band starts to broaden until it spreads completely. At the maximum attained temperatures (~70 °C) that band has almost vanished from the spectrum. During the broadening it is possible to see that extra peaks appear and disappear in the measured spectrum.

The change in the spectrum mentioned in the previous paragraph is also perceived through the frequency spectra of the grating reflection band, measured with the interferometer. Figure 5 shows frequency spectra measured at 20 °C and 70 °C, where it is possible to see the broadening effect at higher temperatures.

A further set of optical spectra is presented in Figure 6, measured more recently. As it can be seen from Figure 6, the spectral behaviour with respect to changes in temperature does not reproduce any of the previously observed characteristics (compare, e.g., with Figure 4). In the later set a single spectral band is observed at room

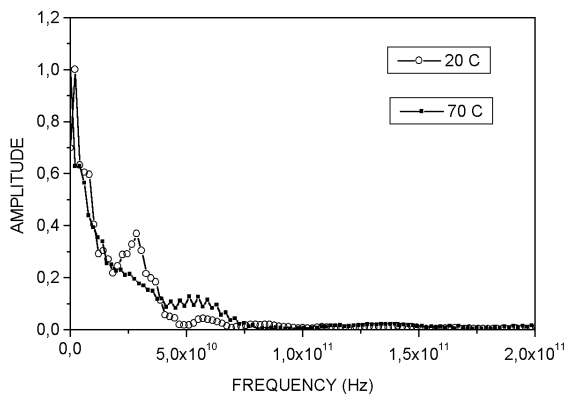


Fig. 5 – Frequency Spectra at 20 °C and 70 °C

temperature. As the temperature increases this reflection band shifts initially to longer wavelengths, while at higher temperatures (T~40°C) it can be seen that a second peak is partially distinguishable at the shorter wavelength tail of the spectrum.

V. DISCUSSION

The second peak in the rejection spectrum of the grating can be due to a ghost grating produced by spurious reflection in the optical path of the recording set up. The difference in the Bragg wavelengths can be assigned to two gratings, one written at a subtle diverse angle, α . The angle

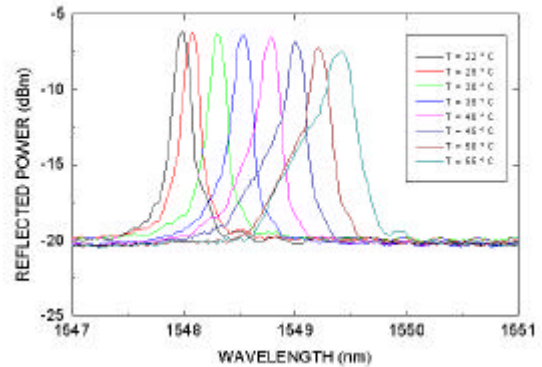


Fig. 6 – Optical response of the same FBG as a function of temperature.

α can be calculated by the grating period, Λ_s , of a slanted structure by [3]:

$$\Lambda_s = \frac{\lambda_s}{2 \cdot n_{eff}} = \frac{\lambda_B}{2 \cdot n_{eff} \cdot \cos(\alpha)} = \frac{\Lambda_B}{\cos(\alpha)}$$

where λ_s is the Bragg wavelength of the slanted grating, Λ_B and λ_B are the grating period and Bragg wavelength at zero angle, respectively, and n_{eff} is the effective index of the guided mode. Using the ratio of the two Bragg wavelengths (zero angle and α)

$\alpha = 0.87^\circ$. This result (~ 52 min of arc) is compatible with a small misalignment in the optical path of the UV writing beam, caused maybe by the adjustment process of the fibre position in the beginning of the writing process. Since the UV laser has a relatively high power, even a short initial exposition might have recorded a grating.

The spectral response of FBG with temperature shows a significant thermal induced strain gradient. In fact, its reflective spectrum was also distorted because of nonuniform changes in both the physical pitch length and the refractive index of the grating.

VI. REFERENCES

- [1] A. Othonos, K. Kalli, Fiber Bragg Gratings, Artech House, New York, 1999.
- [2] I. Abe - Interferômetro híbrido para análise de espectros óticos. Dissertação de Mestrado, CEFET/PR. Curitiba (Brasil), 1998.
- [3] R. Kashyap, Fiber Bragg Grating. Academic Press, New York, 1999.